2015 International Nuclear Atlantic Conference - INAC 2015
São Paulo, SP, Brazil, October 4-9, 2015
ASSOCIAÇÃO BRASILEIRA DE ENERGIA NUCLEAR - ABEN
ISBN: **978-85-99141-06-9**

HEAT EXCHANGER OPTIMIZATION OF A CLOSED BRAYTON CYCLE FOR NUCLEAR SPACE PROPULSION

Guilherme B. Ribeiro, Lamartine N. F. Guimarães and Francisco A. Braz Filho

Divisão de Energia Nuclear - Instituto de Estudos Avançados
Trevo Coronel Aviador José Alberto Albano do Amarante, 1, Putim
12228-001 São José dos Campos, SP
[gbribeiro, guimarae, fbraz]@ieav.cta.br

ABSTRACT

Nuclear power systems turned to space electric propulsion differs strongly from usual ground-based power systems regarding the importance of overall size and weight. For propulsion power systems, weight and efficiency are essential drivers that should be managed during conception phase. Considering that, this paper aims the development of a thermal model of a closed Brayton cycle that applies the thermal conductance of heat exchangers in order to predict the energy conversion performance. The centrifugal-flow turbine and compressor characterization were achieved using algebraic equations from literature data. The binary mixture of He-Xe with molecular weight of 40 g/mole is applied and the impact of heat exchanger optimization in thermodynamic irreversibilities is evaluated in this paper.

1. INTRODUCTION

When compared to ground-based power systems, space power systems present a set of novel aspects, such as low power level, lightweight and a radiant heat rejection from the energy conversion scheme. For propulsion purposes, lighter power systems for the same power output promote more available mass for the payload. Furthermore, the high cost involved in sending the power systems into the space by current launch technologies makes its mass and size critical factors that can constrain the feasibility of nuclear power systems for space propulsion [1]. Therefore, special attention should be focused on these aspects, since they perform high influence on the viability of use of such power systems.

It is known that the Closed Brayton Cycle (CBC) is one of the most promising energy conversion technologies for space power systems, since it results in high energy efficiencies and high power output to radiator area ratio [2]. Additionally, CBC technology combines high energy conversion efficiency with high power output to system mass [3]. Based on these characteristics, energy conversion via CBC has been glimpsed as a strategic technology for space exploration and several studies of conceptual designs of CBC for different electrical power were developed [4-8].

The proposed CBC is described schematically in Figure 1. The generated heat of the fission power system is considered as the heat source of the CBC. The outer space is the heat sink and a large radiator panel is used to remove the heat from the CBC by thermal radiation. The heat radiator panel plays an important role in the power system size, being the largest component. The gas turbine and compressor operate at very high speeds and are attached to the electrical generator on a single shaft. Thus, the turbine work is used to drive the compressor and the excess is available as electrical power output, via the alternator. Part of

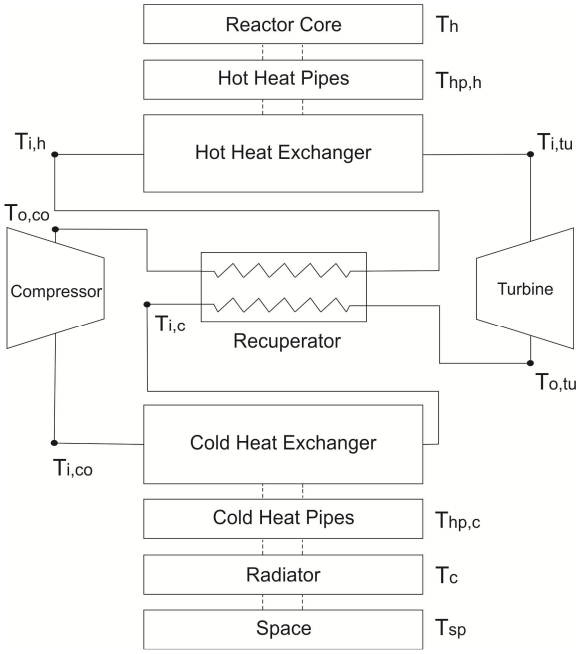

Figure 1: Proposed space power system.

the turbine outlet energy is saved in an internal recuperator by transferring it to the fluid leaving the compressor. The electric power control and protection of the Brayton rotating unit under abrupt changes in the load demand can be performed via a by-pass valve that physically connects the lines of the compressor outlet and turbine inlet. Additionally, the high speed involved in this type of rotating units requires the use of a frequency converter between the electrical generator and the grid.

For ground-based power plants, gas Helium (He) has been selected as working fluid mainly because of its thermo-physical properties and chemical inertness. However, the mixture of He with other noble gases as Xenon (Xe) and Krypton (Kr) produces transport properties that are superior to those of the pure gases with similar molecular weights [9]. Although He has the highest thermal conductivity and the lowest dynamic viscosity of all noble gases, its high turbomachinery loading, and consequently, large size makes pure He nearly impracticable as a working fluid for space power systems. As an example, a He-Xe mixture with molecular weight of 40 g/mole has only 10% of turbomachinery loading and the same heat transfer coefficient, when compared with He [10] (i.e., decreases its size with the same thermal performance). Considering all these aspects, He-Xe mixture is the chosen fluid for this study.

In recent years, much attention has been given to the development of nuclear space power plants. In cases where CBC is considered as the energy conversion method, the performance modelling is commonly based on simplified thermodynamic models where the inlet pressure and temperature of the turbine and compressor were used as input [11-13].

The thermal-hydraulic management of the space reactor core considered in this study is provided by several heat pipes placed inside the core, where these heat pipes are surrounded by packed spheres of uranium nitride (UN) immersed in liquid lead [14]. Figure 2 presents just a portion of a conceptual design of the reactor core where the reactivity control and final assembly is not shown for the sake of simplicity. For very high temperature reactors, heat pipes use sodium as working fluid due to its physical characteristics, since liquid metals present low moderating capabilities and high thermal diffusivities (i.e. low specific heat and

high thermal conductivity). The heat pipes connect the space reactor core to the hot heat exchanger, transferring the heat from the reactor core to the CBC with minimum temperature difference. By the same token, heat pipes are applied to transfer the heat from the cold heat exchanger to the radiator panel. Thus, heat pipes are used as intermediate heat exchangers in order to couple thermally the heat source (reactor core) and the heat sink (space) to the CBC. Figure 3 presents the temperature-entropy diagram of a real CBC applied to space power systems, indicating the same points seen in Figure 1 and with all work and heat transfer rates involved. For the sake of clarity, heat transfer along connecting lines was not included.

It is known from the CBC thermodynamic theory that lower temperature difference encountered at the gas cooler increases the cycle efficiency, as it approaches the system conditions found in the ideal Carnot cycle. Nevertheless, decreasing cold heat exchangers at the expensive of its heat transfer area may turn CBC technology impracticable for space propulsion. For unmanned space applications, heat exchangers present the largest fraction of the total system mass (29.3%) [1]. Thus, a size optimization of both heat exchangers is vital for the design of an efficient and achievable CBC for space exploration purposes.

The purpose of this work is to present a design-based steady state model of a CBC applied for nuclear space reactors. A sensitivity analysis of the sizing of heat exchangers on the final efficiency will be discussed in detail. Furthermore, an optimization approach is suggested in this paper, allowing the match between nuclear power system size and energy conversion efficiency.

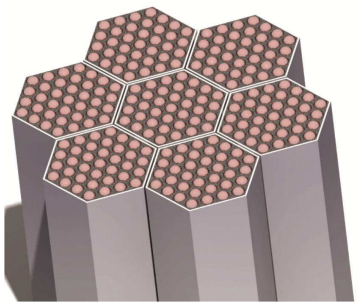

Figure 2: Radial cross-sectional view of heat pipes disposal inside the nuclear reactor core.

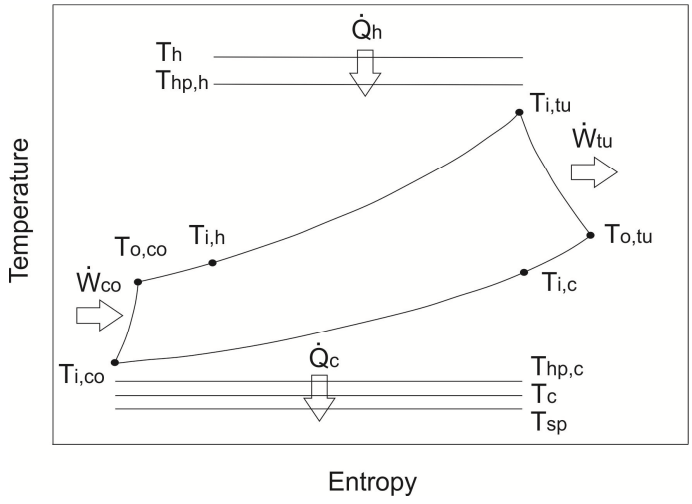

Figure 3: Temperature-Entropy diagram of the Closed Regenerative Brayton Cycle.

2. MODEL DESCRIPTION

2.1. Cycle Components

As described, heat pipes are the components responsible for the heat transport from the reactor core to the hot heat exchanger and from the cold heat exchanger to the radiator panel. Considering these components as heat exchangers with constant thermal conductance and no heat transfer limits, the temperature drop along each heat pipe is proportional to the heat transfer rate and determined as

$$\dot{Q}_h = UA_{hp,h}(T_h - T_{hp,h}) \tag{1}$$

$$\dot{Q}_c = UA_{hp,c}(T_{hp,c} - T_c) \tag{2}$$

where $UA_{hp,h}$ and $UA_{hp,c}$ are the thermal conductance of the hot leg and cold leg heat pipes, respectively. The reactor core thermal power $\dot{Q}_h$ and temperature T_h are input with fixed values, independent of $UA_{hp,h}$. The hot and cold heat exchangers are defined based on effectiveness-NTU method [15]. Thus,

$$\dot{Q}_h = \dot{m}\, c_p \left(T_{hp,h} - T_{i,h}\right)\left[1 - e^{\frac{UA_h}{\dot{m}c_{p,h}}}\right] \tag{3}$$

$$\dot{Q}_c = \dot{m}\, c_p \left(T_{i,c} - T_{hp,c}\right)\left[1 - e^{\frac{UA_c}{\dot{m}c_{p,c}}}\right] \tag{4}$$

where $\dot{m}$ is the gas mass flow rate and UA_h and UA_c are the overall thermal conductance of hot and cold heat exchangers, whereas the specific heat $c_{p,h}$ and $c_{p,c}$ were obtained based on temperatures $T_{i,h}$ and $T_{i,c}$, respectively. The energy balance from the CBC working fluid side is also applied for both heat exchangers as follows

$$\dot{Q}_h = \dot{m}\left(h_{i,tu} - h_{i,h}\right) \tag{5}$$

$$\dot{Q}_c = \dot{m}\left(h_{i,c} - h_{i,co}\right) \tag{6}$$

where $h_{i,tu}$ and $h_{i,comp}$are enthalpies at the turbine and compressor inlet, respectively. The gas enthalpy at the cold heat exchanger inlet $h_{i,c}$ and at the compressor outlet $h_{o,co}$ are obtained consecutively according to the recuperator effectiveness ε_r and its energy balance. Hence,

$$\varepsilon_r = \frac{h_{o,tu} - h_{i,c}}{h_{o,tu} - h_{o,co}} \tag{7}$$

$$h_{i,h} - h_{o,co} = h_{o,tu} - h_{i,c} \tag{8}$$

The turbine and compressor present in the CBC can be defined as polytropic processes with expansion and compressor efficiencies (i.e η_{tu} and η_{co}) as follows

$$\frac{T_{i,tu}}{T_{o,tu}} = PR^{\left(\frac{\gamma_{tu}-1}{\gamma_{tu}}\right)\eta_{tu}} \tag{9}$$

$$\frac{T_{o,co}}{T_{i,co}} = PR^{\left(\frac{\gamma_{co}-1}{\gamma_{co}}\right)\frac{1}{\eta_{co}}} \tag{10}$$

where the terms γ_{tu} and γ_{co} are the specific heat ratios of the working fluid calculated according to $T_{i,tu}$and $T_{i,co}$, respectively. The cycle pressure ratio PR, as well as the turbomachinery shaft speed ratio SR, are obtained via algebraic equations representing the performance map of the turbine and compressor [16]. Fourth-order polynomial regressions with cross-terms were performed based on the turbomachinery available data [17], for a He-Xe mixture of 40 g/mole. Thus,

$$\begin{aligned}\dot{m} = A_{tu} + B_{tu}.PR + C_{tu}.PR^2 + D_{tu}.PR^3 + E_{tu}.SR + F_{tu}.SR^2 + G_{tu}.SR^3 \\ + H_{tu}.PR.SR + I_{tu}.PR^2.SR + J_{tu}.PR.SR^2 + K_{tu}.PR^2.SR^2\end{aligned} \tag{11}$$

$$\begin{aligned}\dot{m} = A_{co} + B_{co}.PR + C_{co}.PR^2 + D_{co}.PR^3 + E_{co}.SR + F_{co}.SR^2 + G_{co}.SR^3 \\ + H_{co}.PR.SR + I_{co}.PR^2.SR + J_{co}.PR.SR^2 + K_{co}.PR^2.SR^2\end{aligned} \tag{12}$$

Likewise, the efficiencies η_{tu} and η_{co} are also calculated algebraically dependent of mass flow rate and speed ratio as

$$\begin{aligned}\eta_{tu} = L_{tu} + M_{tu}.SR + N_{tu}.SR^2 + O_{tu}.SR^3 + P_{tu}.\dot{m} + Q_{tu}.\dot{m}^2 + R_{tu}.\dot{m}^3 \\ + S_{tu}.SR.\dot{m} + T_{tu}.SR^2.\dot{m} + U_{tu}.SR.\dot{m}^2 + V_{tu}.SR^2.\dot{m}^2\end{aligned} \tag{13}$$

$$\begin{aligned}\eta_{co} = L_{co} + M_{co}.SR + N_{co}.SR^2 + O_{co}.SR^3 + P_{co}.\dot{m} + Q_{co}.\dot{m}^2 + R_{co}.\dot{m}^3 \\ + S_{co}.SR.\dot{m} + T_{co}.SR^2.\dot{m} + U_{co}.SR.\dot{m}^2 + V_{co}.SR^2.\dot{m}^2\end{aligned} \tag{14}$$

A coefficient of determination of no less than 98.8% was achieved for all four algebraic equations. Applying these representative equations for an arbitrary mass flow rate, a single value of PR and SR is achieved via Newton-Raphson method. The work resulted from the expansion and compression processes are obtained from the energy balance. Therefore,

$$\dot{W}_{tu} = \dot{m}\left(h_{i,tu} - h_{o,tu}\right) \tag{15}$$

$$\dot{W}_{co} = \dot{m}\left(h_{o,co} - h_{i,co}\right) \tag{16}$$

The radiative heat transfer charged to extract the wasted heat from the cold heat pipe is represented as a fin-tube geometry as follows

$$\dot{Q}_c = \sigma\epsilon A_r \eta_f \left(T_c^4 - T_{sp}^4\right) \tag{17}$$

where σ is the Stefan-Boltzmann constant, ϵ is the radiator emissivity, η_f is the fin efficiency and A_r is the area of radiating surface. The heat sink is represented by the outer space and presents a fixed temperature T_{sp}. The CBC mass flow rate is found iteratively through Newton-Raphson method, where the final solution is achieved when heat transfer rate $\dot{Q}_c$ is obtained from eq. (2) and (17). The arbitrated mass flow rate used to obtain η_{tu} and η_{co} is considered correct when $\dot{Q}_c$ calculated via the cycle energy balance described in Figure 2 matches the value of $\dot{Q}_c$ found from eq. (17). Furthermore, the space power system efficiency is calculated as

$$\eta_{sys} = \frac{\dot{W}_{sys}}{\dot{Q}_h} \tag{18}$$

$$\dot{W}_{sys} = (\dot{W}_{tu} - \dot{W}_{co})\eta_a \tag{19}$$

where η_a represents the alternator efficiency. The entropy generation rate of the CBC is represented as a simple heat-engine operation in contact with two reservoirs [18]. Consequently, the entropy generation rate is interpreted as

$$\dot{S}_{sys} = \frac{\dot{Q}_c}{T_{sp}} - \frac{\dot{Q}_h}{T_h} \tag{20}$$

2.2. Fluid Thermodynamic Properties

Thermodynamic properties of He and Xe were obtained according to NASA library applied for ideal gases [19]. Gases He and Xe under high temperatures ($\geq$ 400 K) and low pressures ($\leq$ 2 MPa) present an ideal gas behavior and the effect of pressure on their compressibility factor, specific heats and transport properties can be neglected [10]. The molecular weight of 40 g/mole corresponds to a molar fraction of approximately 72% and 28% of Helium and Xenon, respectively. Each species was calculated independently, as a function of temperature whereas the He-Xe thermodynamic properties were evaluated within an ideal gas mixture approach.

2.3. Hypotheses and Settings

The model was implemented in the software Engineering Equation Solver – EES [20] to solve the equation set. A thermal power $\dot{Q}_h$ of 160 kW and a surface temperature T_h of 1150 K were considered for the nuclear reactor core, whereas the temperature T_{sp} of 200 K is applied for the outer space. The recuperator effectiveness ε_r was arbitrated in 0.95, typical value for this type of equipment, whereas the alternator efficiency η_a is set in 0.9. It is known that the recuperator mass will weakly vary for different conditions, in order to keep a constant effectiveness. Nevertheless, this effect has been chosen not to be included in this analysis.

In this model, it was assumed that no temperature drop occurs between the heat pipe and the fin root and along the fin set. Hence, a fin efficiency η_f of 1.0 was applied, providing a minimum radiator area A_r, which is the ideal case for propulsion purposes. A typical radiator coating is considered, with a high emittance characteristic. Coatings with emissivity ϵ around

0.9 are usually found for this application [21] and as reference, this same value is employed for this study.

As a reference case, it has been arbitrated for heat pipe thermal conductance a value that represents a temperature drop of 50 K along heat pipes from the hot leg. Similarly, a 50 K temperature difference was applied between heat exchangers outlet and heat pipes as a manner to obtain heat exchangers thermal conductance. As a result of these assumptions, thermal conductances of $UA_{hp,h}$, $UA_{hp,c}$, UA_h and UA_cwere found. Furthermore, a radiator area A_r was chosen in order to satisfy the criteria of 0.3 for the power system efficiency η_{sys}, yielding a total area of 122.4 m^2. Based on these conditions described so far, the reference case was calculated and its inputs and outputs can be seen in tables 1 and 2, respectively.

In this study, it is considered the same type of heat exchanger for both legs and, also, the hypothesis of equal and constant heat transfer coefficient for the heat exchangers is applied. Additionally, it is assumed that the thermal conductances UA_h and UA_c are functions of heat transfer available area and consequently, heat exchanger volume and mass. Therefore, changes on the heat exchanger thermal conductance can be inferred as changes on the heat exchanger mass.

Table 1: Inputs from the reference case.

$\dot{Q}_h$	160 kW
T_h	1150 K
T_{sp}	200 K
ε_r	0.95
ϵ	0.9
η_f	1.0
η_a	0.9
$UA_{hp,h}$	3140 W/K
$UA_{hp,c}$	3140 W/K
UA_h	1430 W/K
UA_c	1139 W/K
A_r	122.4 m^2

Table 2: Outputs from the reference case.

$\dot{Q}_c$	106658 W
$\dot{W}_{tu}$	141972 W
$\dot{W}_{co}$	88631 W
$T_{i,tu}$	1049.0 K
$T_{o,tu}$	906.0 K
$T_{i,c}$	561.0 K
$T_{i,co}$	453.6 K
$T_{o,co}$	542.9 K
$T_{i,h}$	887.9 K
T_c	369.7 K
$T_{hp,h}$	1100.0 K

$T_{hp,c}$	403.6 K
PR	1.471
$\dot{m}$	1.91 kg/s
η_{tu}	0.94
η_{co}	0.86
$\dot{W}_{sys}$	48007 W
η_{sys}	0.3
$\dot{S}_{sys}$	394.16 W/K

3. RESULTS

A sensitivity analysis was performed, where the power system efficiency is evaluated under different components parameters. Figure 4 presents the influence of the hot heat exchanger thermal conductance UA_h on the system efficiency η_{sys}. As can be seen, the increase of thermal conductance provides an increase of the power system efficiency. Moreover, the system efficiency increases asymptotically, reaching a maximum value of 0.32 for the thermal conductance range. According to Figure 4, the design of a hot heat exchanger with UA_h higher than 1500 W/K will not bring worthy results, since a slightly increase of efficiency comes at the expense of strong size and mass changes.

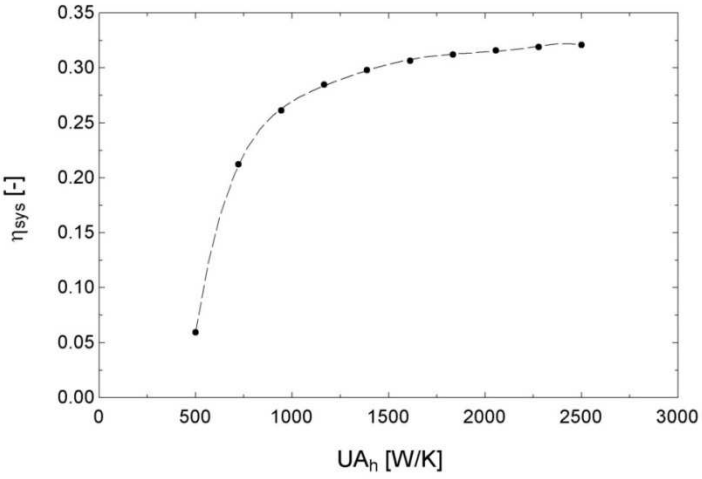

Figure 4: Power system efficiency as function of hot heat exchanger thermal conductance.

Figure 5 shows the influence of the cold heat exchanger thermal conductance UA_c on the system efficiency. Likewise the UA_h, the increase of UA_c resulted in an increase of η_{sys}. Furthermore, a compromise between cold heat exchanger mass and efficiency should also be achieved in a power system conception phase, since higher values of UA_c resulted in a negligible η_{sys} increase. Comparing Figures 4 and 5, it can be seen that higher efficiencies η_{sys} are achievable when the cold heat exchanger is favored with thermal conductance (and consequently mass) increase. For the evaluated range, changes in the UA_h resulted in a maximum η_{sys} of around 0.325, whereas a maximum η_{sys} of 0.35 is obtained varying UA_c.

The entropy generation rate of the nuclear power system $\dot{S}_{sys}$ as function of heat exchanger thermal conductances UA_h and UA_c are shown in Figure 6 and 7, respectively. As expected,

irreversibilities generated through the CBC are minimized with the increase of heat exchanger thermal conductances. These results are in accordance with the behavior of η_{sys} as function of UA_h and UA_c found in Figures 4 and 5. Additionally, it can be concluded that an evaluation based on the second law of thermodynamics is not sufficient for a proper design of power systems turned to propulsion purposes, since it does not take into account the final mass of the system.

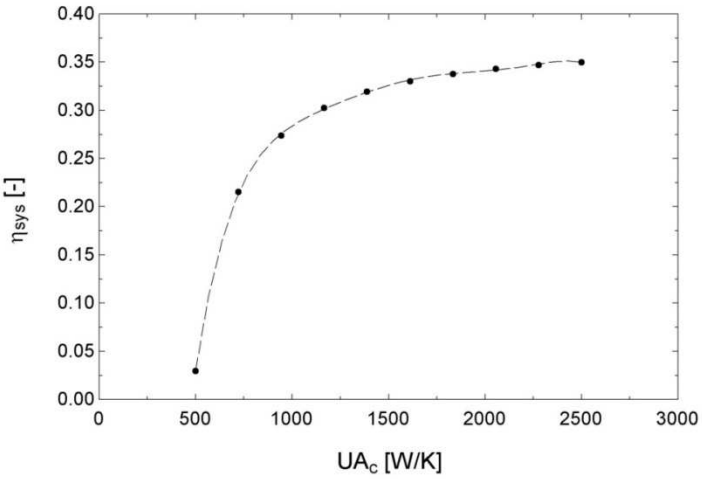

Figure 5: Power system efficiency as function of cold heat exchanger thermal conductance.

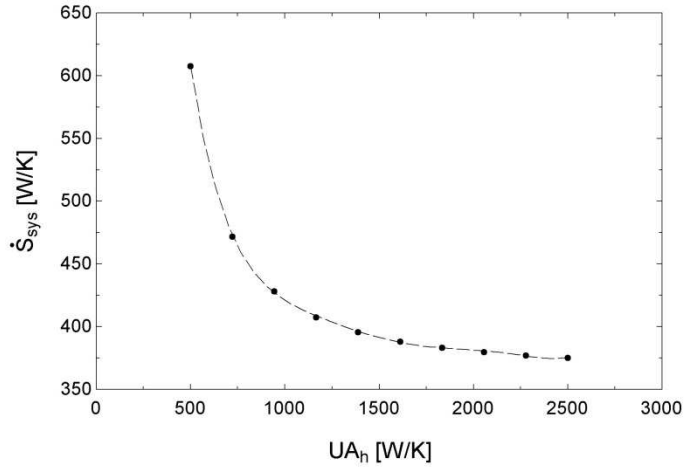

Figure 6: System entropy generation rate as function of hot heat exchanger thermal conductance.

Figure 8 presents the influence of the hot heat exchanger thermal conductance UA_h on the power system efficiency η_{sys} for different sum values of heat exchangers thermal conductance UA_{total} (i.e hot and cold heat exchangers combined). The sum of hot and cold thermal conductance ranged from 2000 to 3500 W/K. As shown in Figure 8, there is a maximum system efficiency for each UA_{total}. Hence, there is a maximum efficiency η_{sys} achievable for a specific total heat exchanger size and mass. Also, according to Figure 8, the maximum efficiency increases with the increasing total heat exchangers mass. Thus, conciliation between total heat exchanger mass and desired system efficiency should be performed during the design phase.

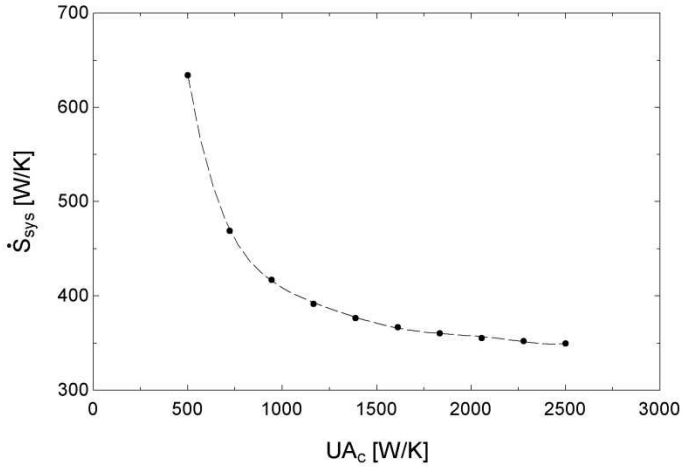

Figure 7: System entropy generation rate as function of cold heat exchanger thermal conductance.

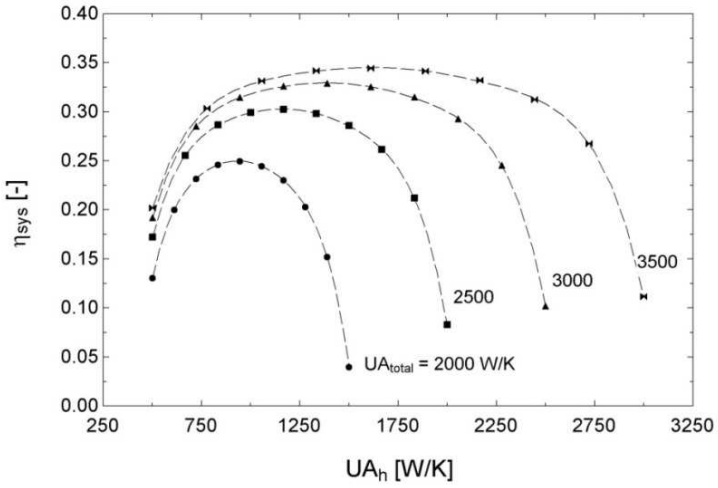

Figure 8: Power system efficiency for different heat exchangers total thermal conductance.

Similarly, the heat exchanger optimization can also be interpreted as the minimization of the entropy generation rate, as shown in Figure 9. As presented in the results, there is a minimum entropy generation rate for a specific total heat exchanger mass. Similarly to Figure 8, the minimum entropy generation rate decreases with the increasing total heat exchangers mass. As expected, for each specific UA_{total}, the optimum heat exchanger thermal conductance UA_h resulted in the highest system efficiency η_{sys} and the lowest entropy generation rate $\dot{S}_{sys}$.

As important as the total heat exchanger mass is the proportion for each heat exchanger and this characteristic should also be considered in order to achieve the optimized efficiency. Therefore, it can be said that a distribution of the heat exchangers mass should be performed in order to accomplish the optimized CBC power system.

The peak values of power system efficiency seen in Figure 8 were plotted as a function of the total heat exchangers thermal conductance in Figure 10. It can be noticed that possible power

systems sizing are positioned below the optimized curve, whereas any point above the optimized curve is not feasible according to the applied size restrictions. Therefore, a space power system should be designed as a manner to place its representative point as close as possible to the optimization boundary.

The reference case considered in this study is shown in Figure 10 and as expected, there is opportunity for a proper optimization. As can be seen, a size optimization can be performed by changing the heat exchangers thermal conductance in order to achieve lower mass for the same power system efficiency. Likewise, heat exchanger thermal conductance can also be changed for efficiency optimization, where the best efficiency is obtained for a constant power system mass.

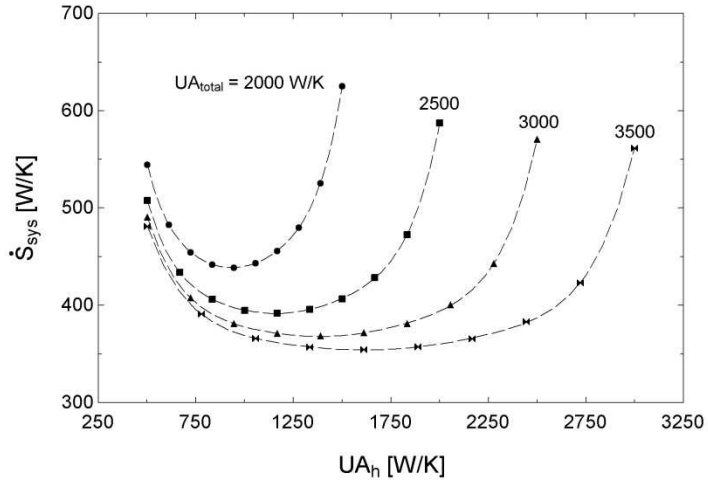

Figure 9: System entropy generation rate for different heat exchangers total thermal conductance.

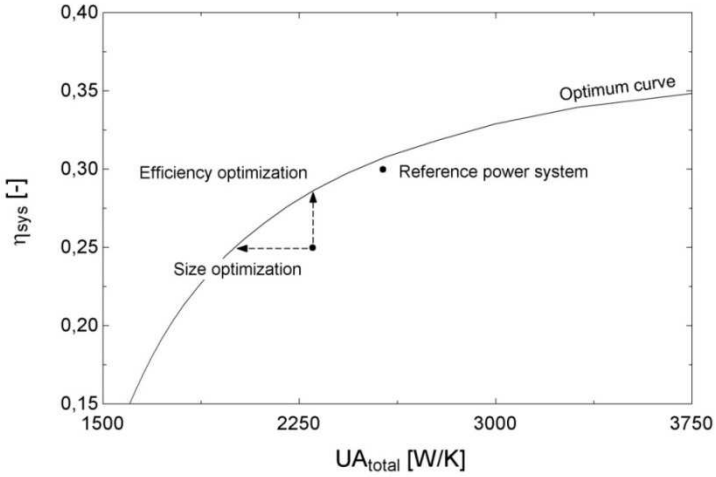

Figure 10: Power system optimization map.

5. COMMENTS AND CONCLUSIONS

A computational model was developed for the thermal prediction of a Closed Brayton Cycle applied for space needs. The model considers global parameters for each component and is

used during the project conception phase, since mass and size are key drivers that allow the use of nuclear energy for aerospace propulsion. A mixture of Helium/Xenon with molecular weight of 40g/mole was applied during this study, using the classic ideal-gas thermodynamic behavior. The turbine and compressor were characterized by algebraic equations obtained from the literature [17].

It was concluded that higher heat exchangers thermal conductance (and consequently, mass) improves the final CBC efficiency. However, a proper matching between cold heat exchanger mass and efficiency should be considered, since the efficiency rate declines for high thermal conductance.

Moreover, it has been concluded that for each total heat exchangers mass (represented by the total thermal conductance), there is a maximum system efficiency and a minimum entropy generation rate. Thus, an efficiency optimization can be performed, changing each heat exchanger proportion on the final volume in order to accomplish the optimized efficiency. By the same token, the size optimization consists in achieving the lowest total heat exchanger volume, while keeping the same system efficiency, by redistributing heat exchangers volume.

6. ACKNOWLEDGEMENT

This study is part of TERRA program (acronym for Advanced Fast Reactors Technology, in Portuguese), sponsored by the Ministry of Defense and Air Force Command. Suggestions and comments of Alexandre D. Caldeira and Roberto D. M. Garcia are highly appreciated.

NOMENCLATURE

$A \cdots V$	=	Coefficients	$\dot{Q}$	=	Heat transfer rate, W
A	=	Area, m^2	SR	=	Speed ratio
c_p	=	Specific heat, J/kg K	$\dot{S}$	=	Entropy generation rate, W/K
h	=	Enthalpy, J/kg	T	=	Temperature, K
$\dot{m}$	=	Mass flow rate, kg/s	UA	=	Thermal conductance, W/K
PR	=	Pressure ratio	$\dot{W}$	=	Work, W

Greek Symbols

ε	=	Recuperator effectiveness	η	=	Efficiency
ϵ	=	Emissivity	σ	=	Stefan-Boltzmann constant
γ	=	Gas specific heat ratio, c_p/c_v			

Subscript

a	=	Alternator	i	=	Inlet
c	=	Cold heat exchanger	r	=	Radiator
co	=	Compressor	sp	=	Space
f	=	Fin	sys	=	System
h	=	Hot heat exchanger	o	=	Outlet
hp	=	Heat pipe	tu		Turbine

REFERENCES

1. Ashe T. L., Baggenstoss W. G., Bons R., "Nuclear Reactor Closed Brayton Cycle Power Conversion System Optimization Trends for Extra-Terrestrial Applications", *Intersociety Energy Conversion Engineering Conference*, Reno, 1990.
2. Tarlecki J., Lior N., Zhang N., "Analysis of Thermal Cycles and Working Fluids for Power Generation in Space", *Energy Conversion & Management*, v. 48, pp. 2864-2878, 2007.
3. El-Genk M. S., "Space Nuclear Reactor Power System Concepts with Static and Dynamic Energy Conversion", *Energy Conversion and Management*, v. 49, pp. 402-411, 2008.
4. Baggenstoss W. G., Ashe T. L., "Mission Design Drivers for Closed Brayton Cycle Space Power Conversion Configuration", *ASME Journal of Engineering for Gas Turbines and Power*, pp. 721-726, 1992.
5. Harty R. B., Otting W. D., Kudija C. T., "Applications of Brayton Cycle Technology to Space Power", *Intersociety Energy Conversion Engineering Conference*, Washington, DC, 1993.
6. Shaltens R. K., Mason L. S., "Early Results from Solar Dynamic Space Power System Testing", *AIAA Journal of Propulsion and Power*, pp. 852-858, 1996.
7. Hyder A. K., Wiley R. L., Halpert G., Flood D. J., Sabripour S., *Spacecraft Power Technologies*, Imperial College Press, London, pp. 332-340,2000.
8. Mason L. S., "A Power Conversion Concept for the Jupiter Icy Moons Orbiter", *International Energy Conversion Engineering Conference*, Reston, 2003.
9. El-Genk M. S., Tournier J. M, "Noble Gas Binary Mixtures for Gas-Cooled Reactor Power Plants", *Nuclear Engineering and Design*, v. 238, pp. 1353-1372, 2008.
10. Tournier J. M., El-Genk M. S., Gallo B. M., "Best Estimates of Binary Gas Mixtures Properties for Closed Brayton Cycle Space Application", *International Energy Conversion Engineering Conference*, San Diego, 2006.
11. Mason L. S., Shaltens R. K., Dolce J. L., Cataldo R. L., "Status of Brayton Cycle Power Conversion Development at NASA GRC", In: El-Genk M. S. editor, *Proceedings of Space Technology and Applications International Forum*, Melville, 2002.
12. Wang J., Gu Y., "Parametric Studies on Different Gas Turbine Cycles for a High Temperature Gas-Cooled Reactor", *Nuclear Engineering and Design*, v. 235, pp. 1761-1772, 2005.
13. Barret M. J., Reid B. M., "System Mass Variation and Entropy Generation in 100-kWe Closed-Brayton-Cycle Space Power Systems", *Space Technology and Applications International Forum*, America Institute of Physics, 2004.
14. Guimarães L. N. F., Camillo G. P., Placco G. M., Barros Jr. A. G., Nascimento J. A., Borges E. M., Lobo P. D. C., "Basic Research and Development Effort to Design a Micro Nuclear Power Plant for Brazilian Space Application", *Journal of British Interplanetary Society*, v. 64, pp. 1-6, 2012.
15. Shah R. K., Sekulic D. P., *Fundamentals of Heat Exchanger Design*, John Wiley & Sons, Hoboken, 2003.
16. Stoecker W. F., *Design of Thermal Systems*, McGraw-Hill, New York, 1980.
17. Gallo B. M., El-Genk M. S., "Brayton Rotating Units for Space Reactor Power Systems", *Energy Conversion and Management*, v. 50, pp. 2210-2232, 2009.
18. Bejan, A., *Advanced Engineering Thermodynamics*, Wiley, New York, 1997.
19. McBride B. J., Zehe M. J., Gordon S., *NASA Glenn Coefficients for Calculating Thermodynamic Properties of Individual Especies*, NASA/TP – 2002 – 211556, 2002.
20. Klein S. A., Alvarado J. L., *Engineering Equation Solver*, F-Chart, 1993.

21. Crosby J. R., *The Development and Qualification of Thermal Controls Coatings for SNAP Systems*, NAA-SR-9908, 1965.